

# Strongly coupled compact lattice QED with staggered fermions

J. Cox, W. Franzki, J. Jersák

*Institut für Theoretische Physik E, RWTH Aachen, Germany*

C. B. Lang

*Institut für Theoretische Physik, Karl-Franzens-Universität Graz, Austria*

T. Neuhaus

*SCRI, Florida State University, Tallahassee, U.S.A.*

---

## Abstract

We explore the compact U(1) lattice gauge theory with staggered fermions and gauge field action  $-\sum_P[\beta \cos(\Theta_P) + \gamma \cos(2\Theta_P)]$ , both for dynamical fermions and in the quenched approximation. ( $\Theta_P$  denotes the plaquette angle.) In simulations with dynamical fermions at various  $\gamma \leq -0.2$  on  $6^4$  lattices we find the energy gap at the phase transition of a size comparable to the pure gauge theory for  $\gamma \leq 0$  on the same lattice, diminishing with decreasing  $\gamma$ . This suggests a second order transition in the thermodynamic limit of the theory with fermions for  $\gamma$  below some finite negative value. Studying the theory on large lattices at  $\gamma = -0.2$  in the quenched approximation by means of the equation of state we find non-Gaussian values of the critical exponents associated with the chiral condensate,  $\beta \simeq 0.32$  and  $\delta \simeq 1.8$ , and determine the scaling function. Furthermore, we evaluate the meson spectrum and study the PCAC relation.

---

## 1 Introduction

Many years of nonperturbative lattice studies have not yet clarified the properties of the strongly coupled QED. Concerning the *noncompact* lattice formulation with staggered fermions the properties of the 2<sup>nd</sup> order phase transition

between the phase with broken chiral symmetry at strong coupling and the symmetric weak coupling (Coulomb) phase are still controversial (see [1–3] and references therein). So is the existence of the conjectured non-Gaussian fixed point which might allow to avoid triviality of QED in the limit of infinite cutoff. The *compact* strongly coupled QED (U(1) gauge theory) with staggered fermions was found to have a phase with broken chiral symmetry, too [4–7]. But the corresponding phase transition to the symmetric phase has not been considered of interest for the continuum theory, as this transition was assumed to be of 1<sup>st</sup> order because of an observed two-state signal on finite lattices [8,9].

There are two reasons to reconsider the order of the phase transition in compact QED. Firstly, a suitable modification of the lattice action might change the order. Such a phenomenon occurs in the pure compact U(1) lattice gauge theory with the extended Wilson action

$$S_U = - \sum_P [\beta \cos(\Theta_P) + \gamma \cos(2\Theta_P)]. \quad (1)$$

( $\Theta_P$  is the plaquette angle proportional to  $F_{\mu\nu}$ . Further details are given in sec. 2.) There the analysis of the decreasing two-state signal [10,11] suggested, that the order of the transition line  $\beta = \beta_c(\gamma)$  changes from the 1<sup>st</sup> to the 2<sup>nd</sup> with decreasing  $\gamma$ . In the full theory with fermions of bare mass  $m_0$  (in lattice units) the two-state signal was found to decrease with decreasing  $\gamma$  for fixed lattice size and  $m_0$ , too [9,12].

Secondly, the recent investigation of the pure U(1) gauge theory with the extended Wilson action [13–15] and the Villain action [16] on finite lattices with sphere-like topology revealed that the two-state signal might in part be due to finite size effects of topological origin. In some range of couplings, when the two-state signal is rather weak, it vanishes when the lattices with sphere-like topology instead of the usual toroidal ones are used, strongly suggesting 2<sup>nd</sup> order in the thermodynamic limit. The two-state signal may be related to certain gauge field configurations, e.g. monopole loops winding around a toroidal lattice. Since the simulations of the full compact QED were performed on cubic lattices with periodic boundary conditions for gauge fields, the same phenomenon should be expected also here, quite independently of the fermions. Thus it may well be that in the thermodynamic limit the two-state signal again vanishes and the phase transition is actually of 2<sup>nd</sup> order.

In this paper we therefore hypothesize that in compact QED with the extended Wilson action and light staggered fermions a part of the phase transition surface (parametrized by  $\gamma$  and  $m_0$ ) is of 2<sup>nd</sup> order. It would be challenging to check this conjecture in simulations with dynamical fermions on lattices with sphere-like topology. Unfortunately, putting fermions on such lattices is

demanding, requiring various preparatory studies, e.g. with free fermions. So presently we are not in the position to make such a direct test.

On the usual toroidal lattices of fixed sizes one can at least investigate, how the two-state signal depends on  $\gamma$  and  $m_0$  and compare its size to that of the pure U(1) gauge theory. Here we report on such a systematic study of the two-state signal on  $6^4$  lattice. The size of the two-state signal can be conveniently characterized by the difference (“gap”)  $\Delta e_P$  between the mean values  $e_P$  of  $\cos(\Theta_P)$  in each of the coexistent states.

A study of the  $\gamma$ -dependence of  $\Delta e_P$  at fixed  $m_0$  was made by Okawa [12] some time ago. He suggested that at  $\gamma = -1.3$  and  $m_0 = 0.1$  the two-state signal is already absent and the transition is therefore of 2<sup>nd</sup> order there. Our present study with larger statistics and a modern hybrid Monte Carlo fermion algorithm shows that the two-state signal persists on the toroidal  $6^4$  lattice even at  $\gamma = -1.5$  (simulations at still smaller  $\gamma$  are prohibitively expensive). However,  $\Delta e_P$  is smaller than in the pure U(1) theory at  $\gamma \simeq -0.5$ , where recent work on spherical lattices [14,15], as well as earlier investigations on toroidal lattices [11] strongly suggest 2<sup>nd</sup> order.

At fixed  $\gamma$  the gap  $\Delta e_P$  increases as  $m_0$  decreases. Since in the continuum limit fermions of finite mass can be obtained only when  $m_0 \rightarrow 0$ , the value of  $\Delta e_P$  at  $m_0 = 0$  must be considered. At  $\gamma = -0.2$  we find that  $\Delta e_P$ , extrapolated to this limit, is of the same magnitude as in the pure gauge theory at  $\gamma = 0$ . Numerical evidence on spherical lattices suggests 2<sup>nd</sup> order in the latter case [13–15]. Thus our results of dynamical fermion calculations on  $6^4$  lattice, described in sec. 3, support the hypothesis that at some negative  $\gamma$  the transition is indeed of 2<sup>nd</sup> order even for light fermions.

If so, then it is justified to consider the continuum limit and investigate its physical properties. We do first steps in this direction, using the quenched approximation. As described in sec. 4, we have studied on toroidal lattices at  $\gamma = -0.2$  the chiral condensate, susceptibilities, equation of state and the meson masses. The data have been obtained in Monte Carlo runs for a simultaneous investigation of the gauge-ball spectrum in the pure U(1) gauge theory in both phases [17]. For that purpose we have accumulated a large number of gauge field configurations at 17  $\beta$ -points on lattices up to  $20^3 40$  (further details are given in [17]). All these points are close to the phase transition, but outside the tunneling region where the two-state signal occurs.

## 2 Action and phase diagram

Compact QED with extended Wilson action for gauge field and staggered fermions on the lattice is defined by the action

$$S = S_\chi + S_U, \quad (2)$$

$$S_\chi = \sum_{x,y} \bar{\chi}_x M_{x,y} \chi_y \quad (3)$$

$$\equiv \frac{1}{2} \sum_x \bar{\chi}_x \sum_{\mu=1}^4 \eta_{x\mu} (U_{x,\mu} \chi_{x+\mu} - U_{x-\mu,\mu}^\dagger \chi_{x-\mu}) + m_0 \sum_x \bar{\chi}_x \chi_x, \quad (4)$$

$$S_U = - \sum_P [\beta \cos(\Theta_P) + \gamma \cos(2\Theta_P)]. \quad (5)$$

Here,  $\Theta_P \in [0, 2\pi)$  is the plaquette angle, i.e. the argument of the product of U(1) link variables around a plaquette  $P$ , and  $\beta$  and  $\gamma$  are the single and the double charge representation couplings, respectively. Taking  $\Theta_P = a^2 g F_{\mu\nu}$ , where  $a$  is the lattice spacing, and  $\beta + 4\gamma = 1/g^2$ , one obtains for  $S_U$  in the limit of weak coupling  $g$  the usual continuum gauge field action  $S = \frac{1}{4} \int d^4x F_{\mu\nu}^2$ . The staggered fermion field  $\chi$  corresponds to four fermion species in the continuum limit. The lattice model has global  $U(1) \otimes U(1)$  chiral symmetry for vanishing fermion bare mass,  $m_0 = 0$ . The limit  $m_0 = \infty$  corresponds to the pure U(1) gauge theory with extended Wilson action.

Throughout this work we consider the theory on hypercubic lattices with periodic boundary conditions in all directions except the antiperiodic boundary condition of the fermion field in one (“time”) direction. We call such lattices “toroidal”.

From the accumulated numerical evidence we know that for any fixed value of  $m_0$  this lattice gauge theory has a line of phase transitions in the  $(\beta, \gamma)$ -plane between the strong coupling confinement phase and the weak coupling Coulomb phase. On finite toroidal lattices it has a two-state signal (gap  $\Delta e_P$ ) in  $\langle \cos \Theta_P \rangle$  in a broad region of  $\gamma$ -values, including  $\gamma = 0$  (Wilson action) [8,9,12,18–20].

These metastability phenomena are similar to those in the pure U(1) lattice theory. The recent studies of that theory on spherical lattices strongly suggest that in spite of non-vanishing  $\Delta e_P$  the order changes at  $\gamma = \gamma_0 \simeq 0$ ,  $\gamma_0$  probably being slightly positive, and is of 2<sup>nd</sup> order for  $\gamma \leq \gamma_0$  [14,15]. In both theories the two-state signal on toroidal lattices weakens with decreasing  $\gamma$ , but is present until the large autocorrelation time at large negative  $\gamma$  makes simulations prohibitively expensive. Thus on toroidal lattices the two-state signal on the phase transition line cannot be avoided. However, an analogy

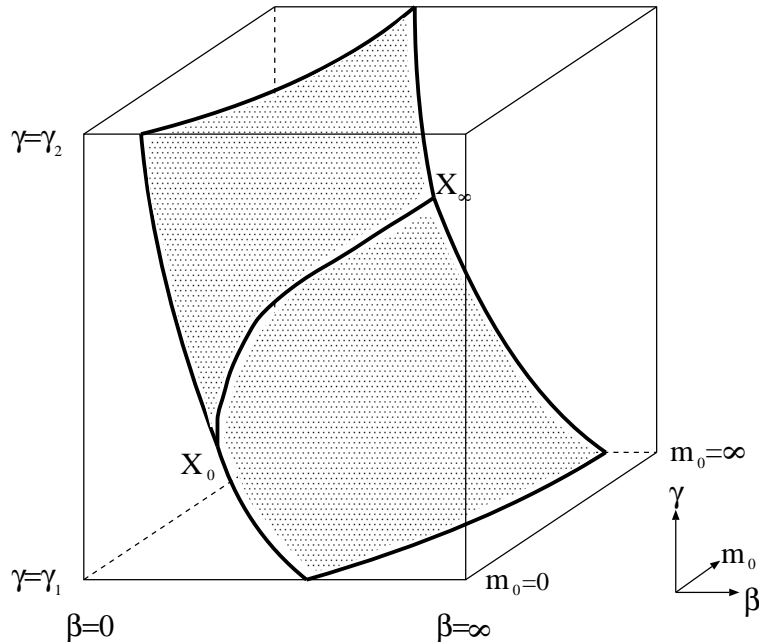


Fig. 1. Expected schematic position and nature of the confinement-Coulomb phase transition sheet in the three-dimensional phase diagram of compact lattice QED with staggered fermions. The sheet of phase transitions is of 1<sup>st</sup> (2<sup>nd</sup>) order above (below) the line  $X_\infty X_0$ . The point  $X_0$  might be at  $\gamma = -\infty$ . The  $\gamma$  axis extends from large negative  $\gamma_1$  to  $\gamma_2 \simeq 0.5$ .

with the pure U(1) theory suggests that in the full theory for any  $m_0 > 0$  the transition becomes 2<sup>nd</sup> order at some *finite* negative value of  $\gamma$ . Fig. 1 shows the conjectured sheet of phase transitions in the thermodynamic limit.

For fixed  $\gamma$  (and  $\beta$  at the transition) the two-state signal increases with decreasing  $m_0$ . Thus the supposed region of 2<sup>nd</sup> order shifts to lower values of  $\gamma$ . Whether the order changes at finite  $\gamma$  also at  $m_0 = 0$  (as suggested in fig 1 by the position of the point  $X_0$ ) is a challenging question.

The continuum limit of the model can be considered at any point of the 2<sup>nd</sup> order surface below the line  $X_\infty X_0$ , as well as at the line itself. We expect that for  $m_0 > 0$  this limit will be in the universality class of the pure gauge theory for the following reason: In the continuum limit the lattice constant  $a$  is determined in physical units (e.g. by fixing some mass in physical units). The fermion bare mass must be expressed in such units too,

$$m_0 = a m_0^{\text{phys}}. \quad (6)$$

For nonzero fixed  $m_0$  the physical fermion mass diverges in the  $a \rightarrow 0$  at nonzero  $m_0$ , and fermions decouple. Thus for  $m_0 > 0$  we expect to find the same non-Gaussian universality class as in the pure gauge theory investigated in [17].

A continuum limit with finite  $m_0^{\text{phys}}$  requires  $m_0 \propto a \rightarrow 0$ . Furthermore, if a chiral symmetric theory  $m_0^{\text{phys}} = 0$  should be constructed, then  $m_0$  must approach zero faster than  $a$ .

It should be pointed out that, if  $\gamma < 0$ , the action (2) does not satisfy reflection positivity. Of course, reflection positivity is a sufficient but not a necessary condition for unitarity, so its absence by itself does not invalidate the investigation of a lattice model for the purpose of quantum field theory. However, it makes it more demanding, as possible sources of unitarity violation must be identified and their scale determined. If they are on the cut-off level, they do no harm, at least if the cut-off can be removed.

In our case the fermionic part of the action is reflection positive and the problem is due to the gauge field action at  $\gamma < 0$ . Numerical investigation of that theory on spherical lattices [14,15] strongly suggest that the critical behaviour at  $\gamma < 0$  and  $\gamma = 0$  belongs to the same universality class. The latter case (Wilson action) is reflection positive, however. Thus the unitarity violations, if any, seem to be confined to small (lattice) distance and do not appear on the physical scale. Of course, this expectation should be tested whenever possible.

### 3 Dynamical fermions: Two-state signal

Here we present our results of dynamical fermion simulations on  $6^4$  toroidal lattice at various values of  $\gamma$  and  $m_0$ , concentrating on  $\gamma < 0$ . The phase transition in the compact QED with light staggered fermions and  $\gamma < 0$  has been studied last quite some time ago [9,12], to our knowledge. The two-state signal was observed down to large negative values of  $\gamma = -1.0$ . The availability of the hybrid Monte Carlo fermion algorithm and larger computer resources suggest the reconsideration of this transition, as it may be crucial for understanding of QED at strong coupling. We work on toroidal lattices like [9,12].

Expecting that the lattice topology contributes substantially to the two-state signal, we put emphasis on the comparison of this signal with the analogous signal in the pure U(1) gauge theory on toroidal lattices. Therefore we study  $e_P$  in both theories under comparable conditions. The values of  $\Delta e_P$  are obtained in the following way: At a chosen value of  $\gamma$  we made simulations at several values of  $\beta$  in the vicinity of the expected phase transition. Inspecting the time evolution of  $e_P$  the  $\beta$  value with clearest two-state signal was chosen. The values and errors of  $\Delta e_P$  have been obtained from a fit of the corresponding histogram with two Gaussians at the distance  $\Delta e_P$ .

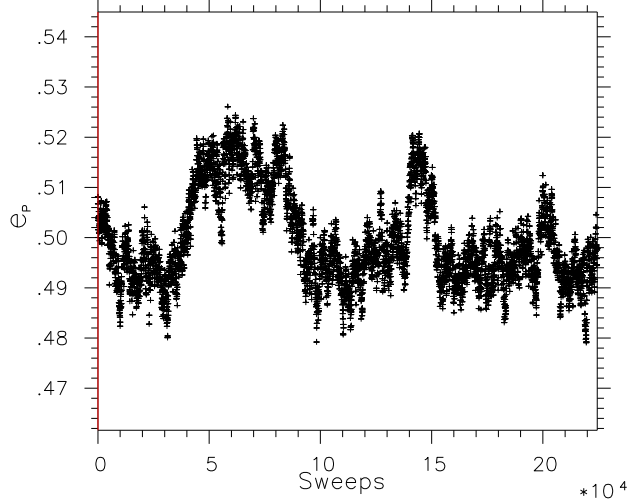


Fig. 2. Time evolution of the plaquette  $e_P$  at  $(\beta, \gamma) = (2.08, -1.3)$  and  $m_0 = 0.1$  on  $6^4$  lattice. Each point represents an average over 100 measurements.

Table 1

Positions of the transition and the size of the gap  $\Delta e_P$  on  $6^4$  lattice in full QED.

$\gamma$	$m_0$	$\beta_c$	$\Delta e_P$	$\gamma$	$m_0$	$\beta_c$	$\Delta e_P$
0	0.1	0.883	0.072(4)	-0.2	0.01	0.970	0.054(2)
-0.2	0.1	1.015	0.047(3)	-0.2	0.02	0.977	0.053(2)
-0.5	0.1	1.240	0.034(2)	-0.2	0.04	0.985	0.054(2)
-1.0	0.1	1.730	0.020(3)	-0.2	0.07	1.000	0.050(4)
-1.3	0.1	2.080	0.018(3)	-0.2	0.10	1.015	0.047(3)
-1.5	0.1	2.350	0.013(2)				

The two-state signal in full QED is clearly observable on  $6^4$  lattice at least until  $\gamma = -1.5$ . The values of  $\Delta e_P$  and the corresponding values of  $\beta_c$  on this lattice are collected in table 1.

As an example we show in fig. 2 the time evolution of  $e_P$  in a run at  $(\beta, \gamma) = (2.08, -1.3)$  and  $m_0 = 0.1$ . The gap between both states is  $\Delta e_P \simeq 0.018$ . The observed tunnelling period indicates that we need very long observation time: the figure represents  $2.2 \times 10^5$  hybrid Monte Carlo trajectories and the lifetime of the metastable states is of the order of  $4 \times 10^4$  trajectories. This explains why the two-state signal was not observed for the same parameters in [12]. It makes also clear that increasing the lattice or further substantial decreasing of  $\gamma$  is prohibitively expensive even today.

The question is whether the two-state signal is a finite size effect or is caused by a genuine 1<sup>st</sup> order transition. Therefore we want to point out the small size of  $\Delta e_P$ : At  $\gamma = -1.3$  and  $m_0 = 0.1$  it is smaller than that in the pure

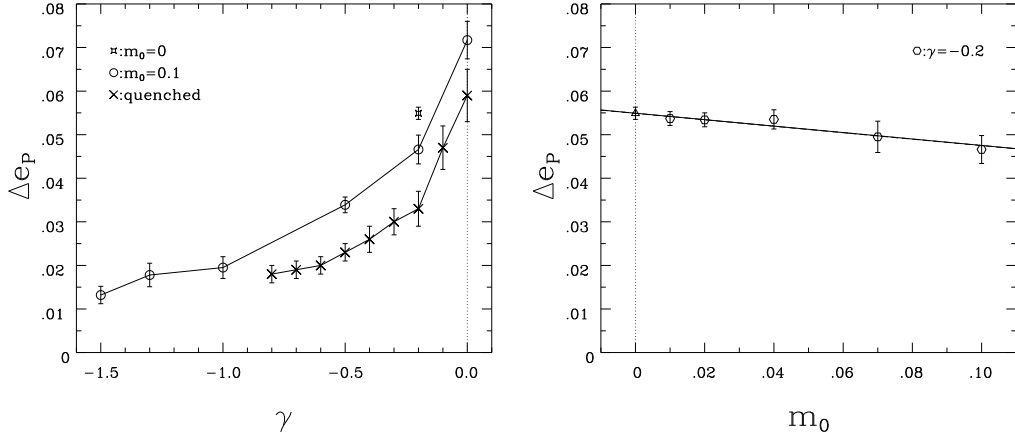


Fig. 3. a) Plaquette discontinuity  $\Delta e_P$  on  $6^4$  lattice as a function of  $\gamma$  in the full QED for  $m_0 = 0.1$  (circles) and in the pure U(1) gauge theory (crosses). At  $\gamma = -0.2$  also the value of  $\Delta e_P$  at  $m_0 = 0$ , obtained by extrapolation, is shown. b) Plaquette gap  $\Delta e_P$  on the same lattice as a function of  $m_0$  in the full QED for  $\gamma = -0.2$ . A linear extrapolation to  $m_0 = 0$  is indicated.

U(1) gauge theory at  $\gamma = -0.5$ , where the 2<sup>nd</sup> order behaviour is clearly seen on spherical lattices [14,15].

Similar observations can be made for  $m_0 = 0.1$  in a broad interval of  $\gamma$  between  $-0.2$  and  $-1.5$ . As is seen in fig. 3a, there the value of  $\Delta e_P$  is smaller than that of the pure U(1) gauge theory at  $\gamma = 0$ . We have also observed that  $\Delta e_P$  in the pure gauge theory roughly agrees with that in the model with fermions of small mass, if compared at identical  $\beta$ .

The investigation of the  $m_0$  dependence of  $\Delta e_P$  becomes very expensive if one approaches small  $m_0$ , even on the small lattice of size  $6^4$ . We have performed such a study at  $\gamma = -0.2$ , with  $m_0$  as small as  $m_0 = 0.01$ . The results are shown in fig. 3b. The increase of  $\Delta e_P$  with decreasing  $m_0$  is moderate and there is no indication of a sudden change at very small  $m_0$ . A linear extrapolation to  $m_0 = 0$ , suggested by the shape of the data, gives  $\Delta e_P \simeq 0.055$ . A quadratic extrapolation gives an insignificantly smaller value. This value still does not exceed the size of the gap in the pure gauge theory at  $\gamma = 0$  on the same lattice.

The comparison of the gap values on  $6^4$  lattice in the theory with dynamical fermions and in pure gauge theory would suggest that even at  $m_0 = 0$  the phase transition may be already of the 2<sup>nd</sup> order at  $\gamma = -0.2$  (since we have arguments, that the pure gauge theory is really second order already at  $\gamma = 0$ ). In spite of our expectation that the gap is caused by gauge fields such a reasoning might be too naive. Nevertheless, it makes plausible our hypothesis that the phase transition at  $m_0 = 0$  becomes 2<sup>nd</sup> order at some finite  $\gamma$ , though possibly smaller than  $\gamma = -0.2$ .



## 4 Quenched approximation

### 4.1 Simulations and fermionic observables

The quenched calculations have been performed at  $\gamma = -0.2$  on large toroidal lattices, typically of the size  $16^3 32$ , at some points up to  $20^3 40$ . We used the configurations produced for the measurement of the gauge-ball masses [17]. We avoided the region very close to the phase transition because of the two-state signal there. This explains a gap in  $\beta$ -values in the data and figures below. In this way we also avoided significant finite size effects.

The transition point in  $\beta$  as determined from the scaling of the gauge-ball masses in the confinement phase at  $\gamma = -0.2$  is  $\beta_c = 1.1607(3)$  [17]. Our following analysis is crucially dependent on a good knowledge of  $\beta_c$  and will be based on this value. We have investigated in both phases the chiral condensate,  $\sigma$  and  $\pi$  susceptibilities and some meson masses. The names of mesons – fermion-antifermion bound states – are chosen in analogy with QCD.

Following standard notation we define the chiral condensate

$$\langle \bar{\chi} \chi \rangle = \langle \text{tr } M^{-1} \rangle \quad (7)$$

and measure it with a Gaussian noise estimator. We also determine the logarithmic derivative  $R_\pi$  of the chiral condensate [21,22]

$$R_\pi = \left. \frac{\partial \ln \langle \bar{\chi} \chi \rangle}{\partial \ln m_0} \right|_{\beta, \kappa} = \frac{m_0}{\langle \bar{\chi} \chi \rangle} \left. \frac{\partial \langle \bar{\chi} \chi \rangle}{\partial m_0} \right|_{\beta, \kappa} . \quad (8)$$

This may be rewritten as a ratio of zero momentum  $\sigma$  and  $\pi$  meson propagators (susceptibilities)

$$\left. \frac{\partial \langle \bar{\chi} \chi \rangle}{\partial m_0} \right|_{\beta, \kappa} = C_\sigma(p=0) , \quad \frac{\langle \bar{\chi} \chi \rangle}{m_0} = C_\pi(p=0) , \quad (9)$$

so that

$$R_\pi = \frac{C_\sigma(p=0)}{C_\pi(p=0)} . \quad (10)$$

The first of eqs. (9) holds in the quenched approximation, if only the connected part of the  $\sigma$  meson propagator is considered. The second is a Ward Identity [23]. The meson operators are defined below.

We expect the validity of the equation of state in analogy with magnetic systems, [21]

$$m_0 = \langle \bar{\chi}\chi \rangle^\delta f(x), \quad x = \frac{t}{\langle \bar{\chi}\chi \rangle^{1/\beta_\chi}}, \quad t = \beta_c - \beta. \quad (11)$$

The suffix  $\chi$  of  $\beta_\chi$  is added to the usual magnetic exponent  $\beta$  to avoid confusion with the coupling  $\beta$ .

A non-vanishing chiral condensate requires a positive zero  $x_0$  of the scaling function  $f(x)$ . The predicted scaling behaviour is

$$\langle \bar{\chi}\chi \rangle = \begin{cases} (t/x_0)^{\beta_\chi} & \text{for } \beta < \beta_c, m_0 = 0, \\ (m_0/f(0))^{1/\delta} & \text{for } \beta = \beta_c, m_0 \neq 0. \end{cases} \quad (12)$$

The equation of state (11) predicts that the ratio  $R_\pi$  depends only on the scaling variable  $x$ ,

$$R_\pi = \left( \delta - \frac{x f'(x)}{\beta_\chi f(x)} \right)^{-1}. \quad (13)$$

The timeslice operators for the mesons (projections to zero momentum) are given by

$$\mathcal{O}^{ik}(t) = \sum_{\vec{x}} s_{\vec{x},t}^{ik} \bar{\chi}_{\vec{x},t} \chi_{\vec{x},t}, \quad (14)$$

with the sign factors  $s_x^{ik}$ ,  $x = \vec{x}, t$ , given in table 2. We measure their correlation functions using point sources and considering only the connected parts. Further details can be found e.g. in [24].

## 4.2 Chiral condensate

The data for the chiral condensate are shown in figs. 4 and 5. In both phases the data turned out to be almost independent of the volume for the  $16^3 32$  and larger lattices we used. Figure 4 exhibits the chiral condensate as a function of  $m_0$  for different  $\beta$  values. To extrapolate the condensate into the chiral limit we made for fixed  $\beta$  in the broken symmetry phase a fit with the ansatz

$$\langle \bar{\chi}\chi \rangle(m_0) = \langle \bar{\chi}\chi \rangle_0 + A m_0 + B m_0 \ln m_0, \quad (15)$$

Table 2

List of measured mesonic operators in the lattice QED with staggered fermions. The continuum quantum numbers  $J^{PC}$  and the name of the corresponding QCD particle are included. The sign factors  $s_x^{ik}$  use the phase factors  $\eta_{\mu x} = (-1)^{x_1+\dots+x_{\mu-1}}$ ,  $\zeta_{\mu x} = (-1)^{x_{\mu+1}+\dots+x_4}$  and  $\varepsilon_x = (-1)^{x_1+\dots+x_4}$ . The index  $s$  and  $a$  at the  $J^{PC}$  are for the singlet and adjoint representation of the flavor symmetry group. The notation follows loosely [24,25].

$i$	$s_x^{ik}$	$J^{PC}$	particle
1	1	$0_s^{++}$ $0_a^{-+}$	$\sigma$ ( $f_0$ ) $\pi^{(1)}$
2	$\eta_{4x}$	$0_a^{+-}$ $0_a^{-+}$	— $\pi^{(2)}$
3	$\eta_{kx}\varepsilon_x\zeta_{kx}$	$1_a^{++}$ $1_a^{--}$	$a_1$ $\rho^{(1)}$
4	$\eta_{4x}\eta_{kx}\varepsilon_x\zeta_{kx}$	$1_a^{+-}$ $1_a^{--}$	$b_1$ $\rho^{(2)}$

motivated by the chiral perturbation theory [26]. In the Coulomb phase we use the ansatz

$$\langle \bar{\chi}\chi \rangle(m_0) = \langle \bar{\chi}\chi \rangle_0 + C(m_0)^z. \quad (16)$$

The value  $\langle \bar{\chi}\chi \rangle_0$  is our estimate for the chiral condensate in the chiral limit. In the confinement phase we get in fact consistent results by both expressions. The exponent  $z$  is nearly independent of  $\beta$ , being  $z \approx 0.8$  in the confinement phase, significantly different from 1. In the Coulomb phase the value is  $z \approx 0.7$  close to the transition and rises with  $\beta$  to  $z \approx 0.8$  at  $\beta = 1.2$ .

The results for  $\langle \bar{\chi}\chi \rangle_0$  are shown in fig. 5 as a function of  $\beta$ . A fit  $ct^{\beta_\chi}$  with  $\beta$  approaching the critical coupling  $\beta_c$  from below results in the value of the magnetic exponent  $\beta_\chi \simeq 0.33$ . The scaling region has been assumed to lie between  $\beta = 1.13$  and  $\beta = 1.16$ . Reducing this interval tends to decrease  $\beta_\chi$ .

### 4.3 Susceptibility ratio $R_\pi$ and equation of state

The study of  $R_\pi$  as suggested in [21] allows for a more sophisticated scaling analysis. As can be seen from (13),  $R_\pi$  should be equal to  $1/\delta$  for  $\beta = \beta_c$ , as long as  $m_0$  is small enough. In the confinement phase with broken chiral symmetry  $R_\pi$  vanishes in the chiral limit, as can be seen from the definition of

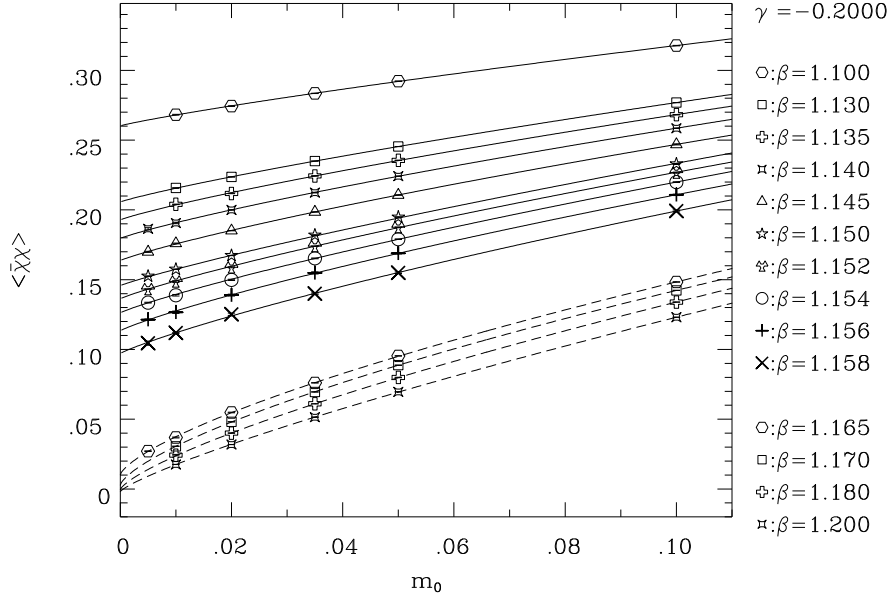


Fig. 4. Chiral condensate on the  $16^3 32$ -lattice as a function of  $m_0$  for different  $\beta$ . The lines are our extrapolation into the chiral limit according to (15) (confinement phase) and (16) (Coulomb phase).

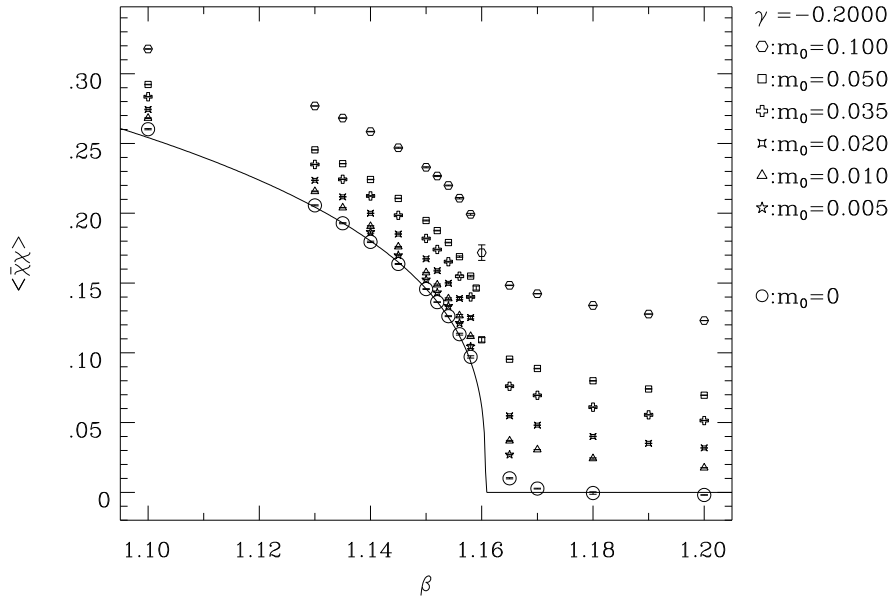


Fig. 5. Chiral condensate on  $16^3 32$ -lattice as a function of  $\beta$ . We show the data for different  $m_0$  and our extrapolation into the chiral limit (circles). The fit has been done according to (12).

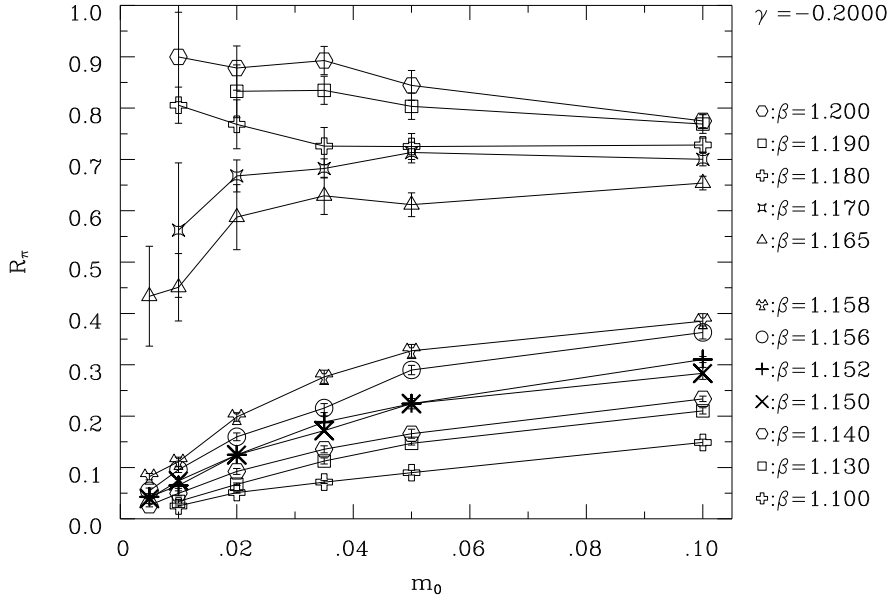


Fig. 6.  $R_\pi$  as a function of  $m_0$  for different  $\beta$  on  $16^3 32$  lattice. The lines connecting the points at the same  $\beta$  are drawn to guide the eye.

$R_\pi$ . In the symmetric phase  $\sigma$  and  $\pi$  meson masses are degenerate, and thus  $R_\pi = 1$  in the chiral limit. The curve of constant  $R_\pi$  separates two groups of curves. It provides an estimate of the critical coupling and  $1/\delta$ .

In both phases the data for  $R_\pi$  are again almost independent of the volume for the  $16^3 32$  and larger lattices, thus we show in fig. 6 the data for  $16^3 32$  lattice only. Since no simulation close to the critical coupling could be done, our estimate for  $\delta$  with this method is bound to have a large uncertainty. From the value of  $R_\pi$  at  $m_0 = 0.05$  for the  $\beta$ -values closest to the phase transition in each phase we find  $\delta = 1.7 - 3.3$ . The mean-field value would be  $\delta = 3$ .

In the symmetric phase all curves should run towards  $R_\pi = 1$ . Our data do not show this behaviour in a clear way. However, in particular at small  $m_0$ , we observe large statistical errors near the transition point. Also, the expectations of chiral symmetry restoration by mass symmetry of parity partners may not hold in the quenched approximation.

To check the validity of the equation of state we also investigate the dependence of  $R_\pi$  on the scaling variable  $x$  in the confinement phase, which is predicted by (13) to be the only parameter. This is done by determining  $\beta_\chi$  by the requirement that all data for  $R_\pi$  lie on a single curve depending only on  $x$ . We get the best results for  $\beta_\chi = 0.32(2)$  (fig. 7a), which is in good agreement with the result obtained from the scaling of the chiral condensate. Varying  $\beta_c = 1.1607(3)$  within its error bars neither improves the independence on  $x$

nor changes  $\beta_\chi$  significantly.

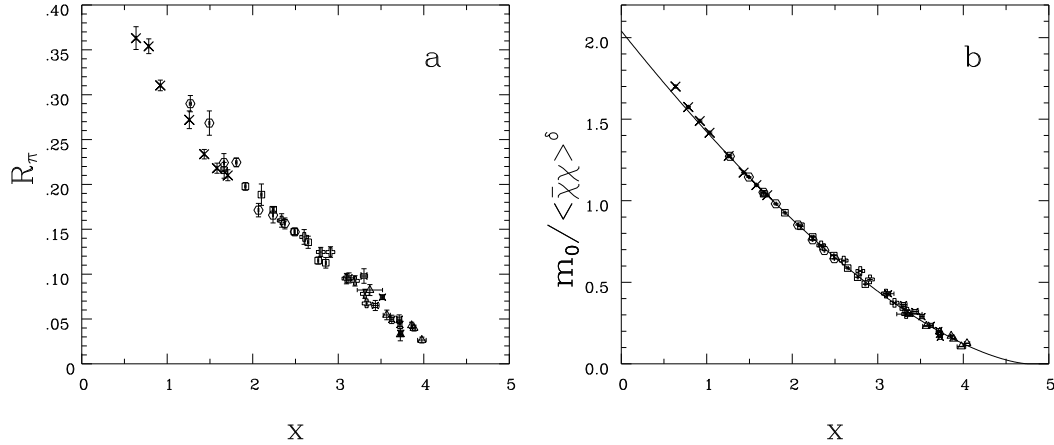


Fig. 7. (a)  $R_\pi(x)$  and (b)  $f(x) = m_0 \langle \bar{\chi}\chi \rangle^{-\delta}$  as functions of the scaling variable  $x = t / \langle \bar{\chi}\chi \rangle^{-1/\beta_\chi}$  on  $16^3 32$  lattice for the exponents  $\beta_\chi = 0.32$  and  $\delta = 1.82$ . The method to obtain these plots and the curve in (b) are discussed in the text.

To determine the exponent  $\delta$  more precisely, we use the fact, that  $f(x)$  should be a function of  $x$  alone. With (11) as an indirect definition for  $f$  and taking our best estimate for  $\beta_\chi = 0.32$  we tune  $\delta$  so that  $m_0 \langle \bar{\chi}\chi \rangle^{-\delta}$  depends only on  $x$ . As shown in figure 7b, this leads to an excellent description of the data with  $\delta = 1.82(10)$ . The result for  $\delta$  is substantially more precise than the above attempt to use  $R_\pi$  directly. If this analysis is done with a slightly different  $\beta_\chi$ , the obtained results are much worse, and no unique value of  $\delta$  could be obtained. The scaling function  $f(x)$  can be very well parameterized as  $f(x) = 0.207(4.68 - x)^{1.49}$ , which is drawn in fig. 7b.

Both exponents determined by this method,  $\beta_\chi = 0.32(2)$  and  $\delta = 1.82(10)$ , differ from corresponding mean field values. The results therefore indicate that this model might have a non-Gaussian fixed point. They may be considered as a first hint that the full compact QED is nontrivial. However, we cannot give a reliable estimate of the systematic errors. We note that  $\frac{1}{4}\beta_\chi(\delta + 1) = 0.23(2)$ , which does not agree with the value  $\nu = 0.35$  as would be expected from the hyperscaling relation.

#### 4.4 Meson spectrum

The masses have been determined with the usual cosh-fits to the connected propagators [27]. Each of the four (cf. table 2) correlations functions  $C^i(t)$  contains signals from both parity states (with the only exception of the pion in the channel  $i = 2$ ) and therefore is fitted to the form

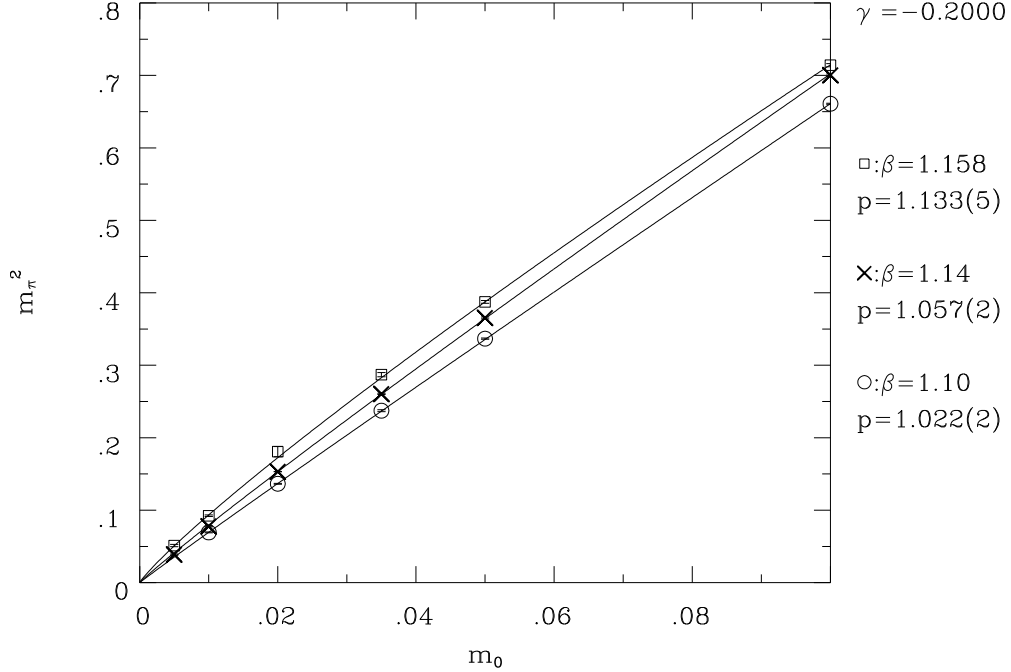


Fig. 8. The figure shows  $m_\pi^2$  vs.  $m_0$  for  $\beta = 1.10$  (circles), 1.14 (crosses) and 1.158 (squares); the fit  $(m_\pi)^2 \propto (m_0)^p$  gives values of  $p$  close to one.

$$\begin{aligned}
B^+ + (-1)^t B^- + \sum_{n=1}^{n^+} A_n^+ \left( e^{-E_n^+ t} + e^{-E_n^+ (L_t - t)} \right) \\
+ (-1)^t \sum_{n=1}^{n^-} A_n^- \left( e^{-E_n^- t} + e^{-E_n^- (L_t - t)} \right) . \quad (17)
\end{aligned}$$

Significant mass determination could be obtained in the  $\sigma, \pi^{(2)}, a_1, \rho^{(1)}$  and  $\rho^{(2)}$  channels. For them, respectively, the numbers of energy levels ( $n^+, n^-$ ) considered were in the confinement phase (1,1), (0,2), (1,1), (2,1), (1,2) and in the Coulomb phase (2,1), (0,2), (2,1), (2,1), (1,2). The lowest energy level was interpreted as the mass of the corresponding particle state. Statistical fluctuations prevent a reliable determination of  $\pi^{(1)}$  and  $b_1$ .

#### 4.4.1 Confinement phase

In the confinement phase finite volume effects become small already at lattice sizes  $12^3 24$ ; we therefore discuss meson masses obtained on  $16^3 32$  lattice only. We note that in this phase the values of both parameters  $B^\pm$  obtained by the fits are consistent with zero.

Close to the chiral limit one expects

$$(m_\pi)^2 \propto m_0 . \quad (18)$$

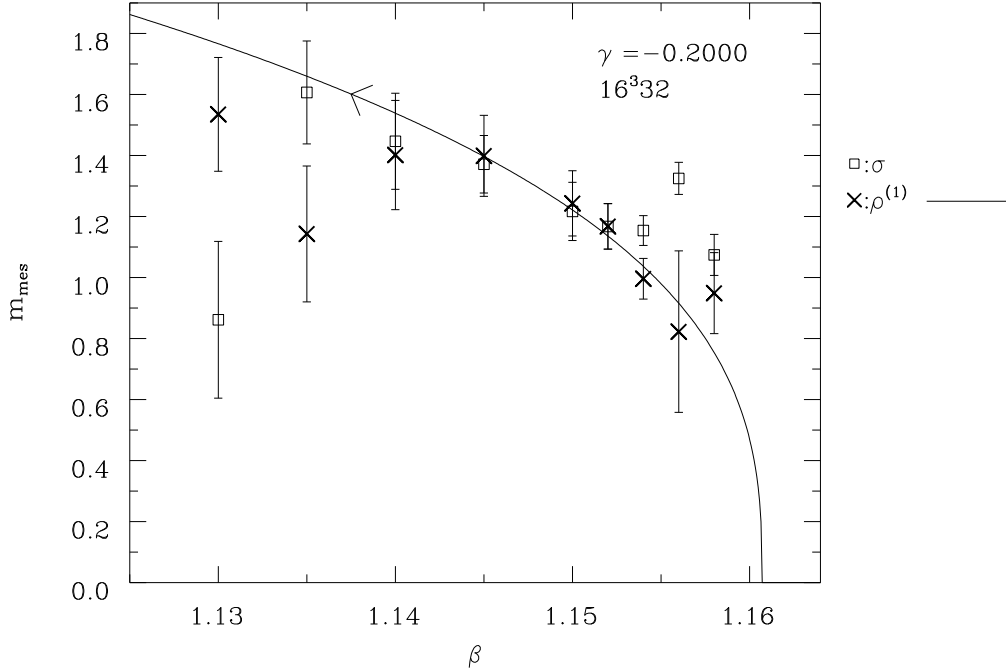


Fig. 9. Masses of  $\sigma$  (squares) and  $\rho^{(1)}$  (crosses) extrapolated to  $m_0 = 0$ . The curve is  $m = ct^{0.35}$ , with fitted  $c$ .

In quenched studies there may be corrections due to so-called chiral logarithms [28–30], thus we fit our results (fig. 8) to  $(m_\pi)^2 \propto (m_0)^p$ . We find values of  $p$  close to one (between 1.02 and 1.13 close to the phase transition).

The  $m_0$  dependence of the non-Goldstone state masses has been parameterized linearly,  $m \propto m_0 + \text{const}$ , as usual. Fig. 9 gives the values of  $\sigma$  and  $\rho^{(1)}$  as they emerge from the extrapolation to  $m_0 = 0$ . The mass of  $\rho^{(2)}$  is compatible with that of  $\rho^{(1)}$ . The  $a_1$  is heavy ( $m > 1.5$ ) and seems not to scale at the phase transition.

The data is not good enough to warrant a fit to a critical exponent. However, assuming the non-Gaussian value  $\nu = 0.35$  obtained in [14,15,17] and the knowledge of  $\beta_c$ , a fit  $m = ct^\nu$  of the  $\rho^{(1)}$ -mass is shown in the plot fig. 9 to be compatible with the data. The  $\sigma$  has mass values of the same order of magnitude as the  $\rho$  whereas the  $a_1$  is definitely heavier by almost a factor of 2.

Comparing the  $\rho$  and  $\sigma$  with the the gauge-balls (determined from the same runs in [17]) we find meson masses quite close to the  $T_1^{+-}$  gauge-ball group. For example, the amplitude of  $\rho$  is  $c = 6.0(2)$  and the corresponding  $T_1^{+-}$ -gauge-ball amplitude is  $5.4(3)$ .



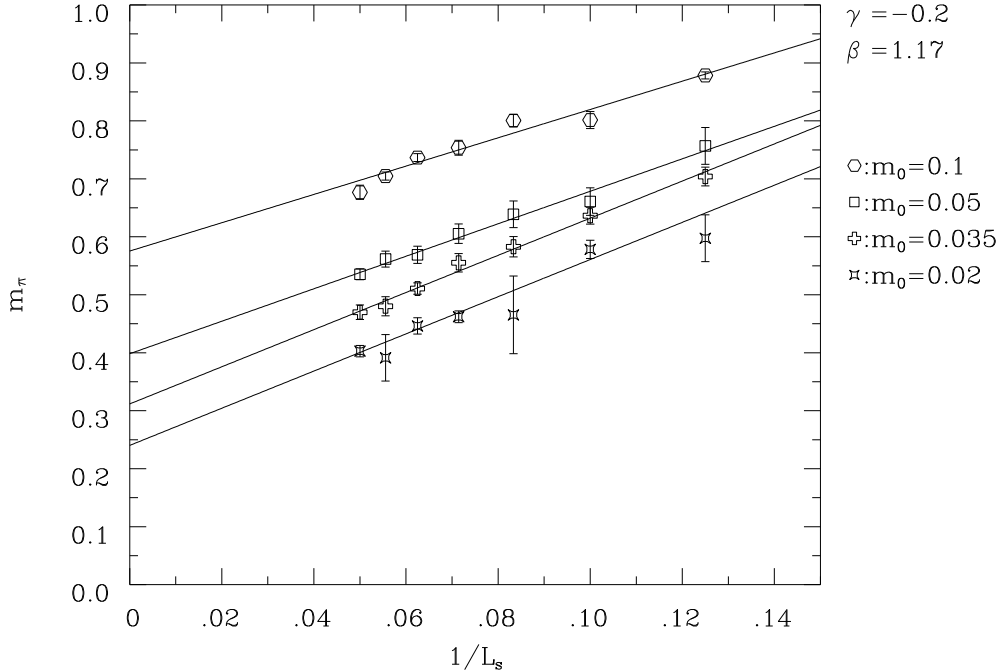


Fig. 10. The  $\pi$  mass in the Coulomb phase at  $\beta = 1.17$  plotted vs.  $1/L_s$  for various  $m_0$ .

#### 4.4.2 Coulomb phase

In the Coulomb phase we expect and we do find sizeable finite volume dependence, presumably caused by massless photons and light fermions. The mesons are therefore expected to be resonances. This is like in the recent study of gauge-ball masses in the Coulomb phase [17]. The volume dependence there was explained as a signal of multi-photon states, but a reliable quantitative extrapolation to the thermodynamic limit was not possible. For mesons the situation is even worse. In particular the Bohr radius, proportional to the inverse fermion mass (which we have not determined), might be much larger than the lattice. Therefore our investigation of the spectrum in the Coulomb phase has only an exploratory character, checking whether unexpected phenomena might be seen in the Coulomb phase close to the phase transition to the confinement phase.

Fig. 10 indicates, that the size dependence may follow a linear  $1/L_s$  behaviour. Using the correspondingly extrapolated values for the pion (para-onium) mass, we obtain fig. 11. For increasing fermion masses one expects  $m_\pi \simeq 2m_0$ , i.e. twice the mass of the constituents. For small constituent mass, one would expect  $m_\pi \propto m_0$  like the positronium spectrum. However, it is not completely excluded that the massless QED in the Coulomb phase at strong coupling shows some nonperturbative phenomena due to IR singularities.

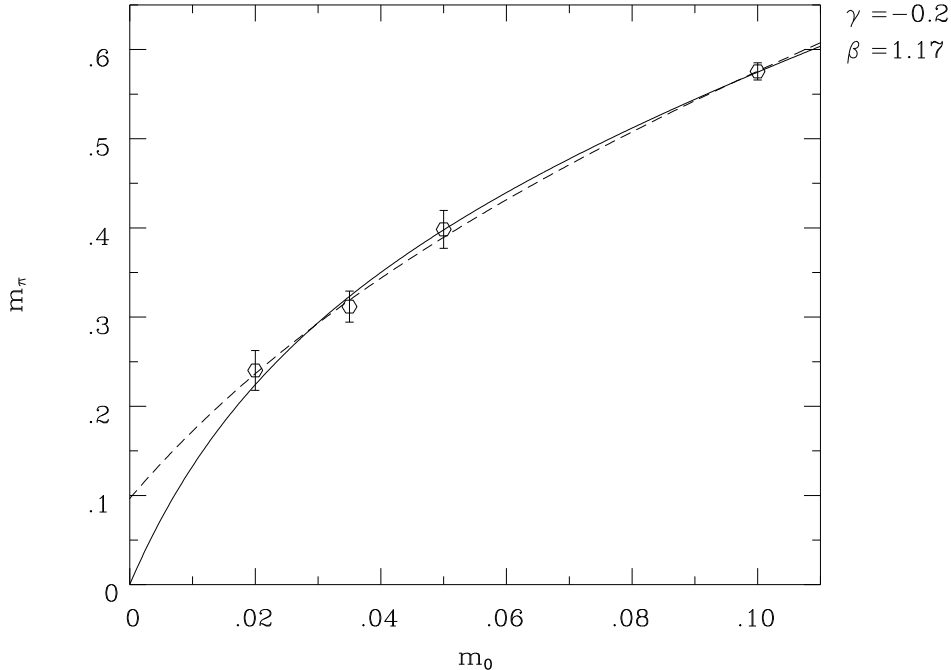


Fig. 11. The values of  $m_\pi$  extrapolated to infinite volume against  $m_0$ . We also show the results of fits (19) with (solid line) and without constraint  $A = 0$ .

Therefore we have fitted the mass values with a simple three-parameter curve

$$m_\pi = \frac{A + Bm_0 + 2m_0^2}{C + m_0} \quad (19)$$

either keeping  $A$  fixed to 0 (solid line in fig. 11) or letting  $A$  free (dashed line,  $A = 0.1(1)$ ). We found, that the data are compatible with both, vanishing and non-vanishing values of  $m_\pi$  at  $m_0 = 0$ , and the conventional expectation of vanishing meson masses is in agreement with the data. The non-vanishing value would imply a decoupling of the corresponding state in the continuum theory if we require that a continuum limit should be taken at  $\beta \rightarrow \beta_c$  and  $m_0 \rightarrow 0$ .

Comparing the mass values for all states as obtained on a fixed lattice size  $16^3 32$  we observe an approximate mass degeneracy of the chiral partners  $\sigma$  and  $\pi$  even at finite  $m_0$ , consistent with chiral symmetry in the  $m_0 = 0$  limit. This is in agreement with the discussion of  $R_\pi$  approaching 1. Also  $\rho^{(2)}$  and  $a_1$  masses are close to each other and to the  $\sigma$  and  $\pi$  masses. Thus the data do not show any significant fine or hyperfine splitting.

This explorative study of the spectrum indicates that much better data and understanding of finite size effects are required to obtain results for the spectrum in the Coulomb phase which would bring further insight.

## 5 Summary

We have studied the compact U(1) gauge theory with staggered fermions on toroidal lattices on both sides of the phase transition line in the  $(\beta, \gamma)$ -plane.

- With dynamical fermions the observed gap  $\Delta e_P$  on  $6^4$ -lattices increases with respect to the pure gauge theory, decreases with decreasing  $\gamma$  but does not vanish in the considered domain  $-1.5 \leq \gamma \leq 0$ . At  $\gamma = -0.2$  and for massless fermions it is of the same size as for the pure gauge theory at  $\gamma = 0$ . Since there the gap disappears on sphere-like lattices we conjecture, that also the fermionic theory may in fact have a critical phase transition at negative  $\gamma$ .
- On large lattices we study the chiral condensate and the meson spectrum in the quenched approximation. Quenched results should not be over-interpreted. We hope, however, that these results stimulate further studies of the compact lattice QED with dynamical fermions.
- The chiral condensate is determined with high precision. The main result of our study is the observation that the chiral condensate can be very well described as a function of both parameters,  $\beta$  and  $m_0$ , by means of an equation of state with the relevant critical indices that have non-Gaussian values:  $\beta \simeq 0.32$  and  $\delta \simeq 1.8$ .
- In the confinement phase we observe chiral symmetry breaking and Goldstone-boson behaviour of the pion, as expected. The mass squared obeys a PCAC behaviour. All masses (extrapolated to vanishing bare fermion mass) have a behaviour compatible with a non-Gaussian scaling at the phase transition in  $\beta$ .
- The results for masses in the confinement phase are generally of better statistical quality than the Coulomb phase results. In the Coulomb phase the masses of the pion and other states are of comparable size.

We obtained a better insight into some aspects of compact lattice QED, in particular concerning chiral symmetry breaking and the meson spectrum in the confinement phase. However, higher statistics will be necessary to improve the quality of some of our results in this phase and to determine the scaling behaviour of the meson masses. In the Coulomb phase not only considerably higher statistics, but also understanding of finite size effects of various origin is required. Here the problems are similar to those of the noncompact QED, except that  $\beta_c$  can be determined from the other, technically simpler phase. This might be an advantage of the compact formulation.

## Acknowledgements

We thank M. Göckeler for reading the manuscript and useful comments and M.-P. Lombardo for discussions. The computations have been performed on the CRAY-YMP and CRAY-T90 of HLRZ Jülich. J.C., W.F. and J.J. thank HLRZ, and T.N. thanks SCRI for the hospitality. The work was supported by DFG.

## References

- [1] S. J. Hands, A. Kocić, J. B. Kogut, R. L. Renken, D. K. Sinclair, and K. C. Wang, *Nucl. Phys.* **B413** (1994) 503.
- [2] V. Azcoiti, G. Di Carlo, A. Galante, A. F. Grillo, V. Laliena, and C. E. Piedrafita, *Phys. Lett.* **379B** (1996) 179.
- [3] M. Göckeler, R. Horsley, V. Linke, P. E. L. Rakow, G. Schierholz, and H. Stüben, *Nucl. Phys.* **B487** (1997) 313.
- [4] V. Azcoiti, A. Cruz, E. Dagotto, A. Moreo, and A. Lugo, *Phys. Lett.* **175B** (1986) 202.
- [5] M. Salmhofer and E. Seiler, *Lett. Math. Phys.* **21** (1991) 13.
- [6] M. Salmhofer and E. Seiler, *Commun. Math. Phys.* **139** (1991) 395.
- [7] H. Gausterer and C. B. Lang, *Phys. Lett.* **263B** (1991) 476.
- [8] J. B. Kogut and E. Dagotto, *Phys. Rev. Lett.* **59** (1987) 617.
- [9] E. Dagotto and J. B. Kogut, *Nucl. Phys.* **B295** [FS21] (1988) 123.
- [10] G. Bhanot, *Nucl. Phys.* **B205** [FS5] (1982) 168.
- [11] H. G. Evertz, J. Jersák, T. Neuhaus, and P. M. Zerwas, *Nucl. Phys.* **B251** [FS13] (1985) 279.
- [12] M. Okawa, *Phys. Rev. Lett.* **62** (1989) 1224.
- [13] C. B. Lang and T. Neuhaus, *Nucl. Phys.* **B431** (1994) 119.
- [14] J. Jersák, C. B. Lang, and T. Neuhaus, *Phys. Rev. Lett.* **77** (1996) 1933.
- [15] J. Jersák, C. B. Lang, and T. Neuhaus, *Phys. Rev.* **D54** (1996) 6909.
- [16] C. B. Lang and P. Petreczky, *Phys. Lett.* **387B** (1996) 558.
- [17] J. Cox, W. Franzki, J. Jersák, C. B. Lang, T. Neuhaus, and P. W. Stephenson, *Gauge-ball spectrum of the four-dimensional pure  $U(1)$  gauge theory*, HLRZ 84/96, to be published in Nucl. Phys. B.

- [18] V. Azcoiti, G. Di Carlo, and A. F. Grillo, *Phys. Rev. Lett.* **65** (1990) 2239.
- [19] V. Azcoiti, A. Cruz, G. Di Carlo, A. F. Grillo, and A. Vladikas, *Phys. Rev.* **D43** (1991) 3487.
- [20] V. Azcoiti, I. M. Barbour, R. Burioni, G. Di Carlo, A. F. Grillo, and G. Salina, *Phys. Rev.* **D51** (1995) 5199.
- [21] A. Kocić, J. B. Kogut, and M.-P. Lombardo, *Nucl. Phys.* **B398** (1993) 376.
- [22] M. Göckeler, R. Horsley, P. E. L. Rakow, G. Schierholz, and H. Stüben, *Nucl. Phys. B (Proc. Suppl.)* **34** (1994) 527.
- [23] G. W. Kilcup and S. R. Sharpe, *Nucl. Phys.* **B283** (1987) 493.
- [24] M. F. L. Golterman, *Nucl. Phys.* **B273** (1986) 663.
- [25] R. Altmeyer, K. D. Born, M. Göckeler, R. Horsley, E. Laermann, and G. Schierholz, *Nucl. Phys.* **B389** (1993) 445.
- [26] J. Gasser and H. Leutwyler, *Phys. Lett.* **184B** (1987) 83.
- [27] A. Ali Khan, M. Göckeler, R. Horsley, P. E. L. Rakow, G. Schierholz, and H. Stüben, *Phys. Rev.* **D51** (1995) 3751.
- [28] C. W. Bernard and M. F. L. Golterman, *Phys. Rev.* **D46** (1992) 853.
- [29] S. R. Sharpe, *Phys. Rev.* **D46** (1992) 3146.
- [30] R. D. Mawhinney, *Nucl. Phys. B (Proc. Suppl.)* **47** (1996) 557.